How to cite: *Angew. Chem. Int. Ed.* **2025**, e202421289
doi.org/10.1002/anie.202421289

Organic Photovoltaics

Highly Efficient Acceptors with a Nonaromatic Thianthrene Central Core for Organic Photovoltaics

Zheng Xu[+], Xiangjian Cao[+], Zhaoyang Yao, Wenkai Zhao, Wendi Shi, Xingqi Bi, Yu Li, Yaxiao Guo, Guanghui Li, Guankui Long, Xiangjian Wan, Chenxi Li, and Yongsheng Chen**

Abstract: Despite the great role in determining molecular packings and organic photovoltaic outcomes, very rare candidates could be employed as central cores in current high-performance acceptors except diimide-based moieties. Herein, a new type of central core of nonaromatic thianthrene is explored firstly, affording an exotic but structurally tailorable molecular platform for acceptor design. A unique puckered rather than planar conformation of central core is adopted, caused by the 4n πe^- feature, great ring strain and largely the insufficient p–π orbital overlap of lone pair on sulfur of thianthrene and coterminous benzene planes. As a result, the absorption of thianthrene-based acceptors (CS1, CS2, and CS3) shows unexpected blue shift comparing to the phenazine-based counterpart (CH20), regardless of the intrinsically strong electron-donating characteristic of low valence sulfur atoms. Even so, the desired molecular packing and fibrillary film morphology, assisted by the suitable chlorination on thianthrene, still contribute to the best device efficiency of 19.0% based on D18:CS2 blends. Such novel work renders an underdeveloped NFA platform with the potentials for achieving PCE of over 20%.

Introduction

Organic photovoltaics have undergone a rapid increase in power conversion efficiency (PCE) in the last few years and reached a breakthrough in PCE of more than 20% currently.[1–11] The greatest contribution for such a surging development comes from the unremitting exploration of innovative organic light-harvesting materials.[12–19] Among them, the design of high-performance non-fullerene acceptors (NFAs) is crucially important but quite challengeable as well.[20–26] Because NFAs in active layers are in charge of harvesting low-energy photons, which is not only essential for matching the spectrum of sunlight better[27–29] but also makes NFAs severely restricted by the "energy gap law."[30,31] For the high-performance Y-series NFAs, a more compact and ordered 3D molecular packing network is well established comparing to other type of NFAs.[32–34] This helps NFAs to escape the limitations of the "energy gap law" through delocalizing molecular vibrations on neighboring stacked molecules,[35–37] especially for the near-infrared (NIR) NFAs. More excitingly, such a favorable feature is expected to be enhanced if further improving molecular packing strength and ordering through innovative structural exploration,[38,39] for example, extending central units to two dimensions[40,41] given the irreplaceable role of central core in determining molecular packing modes and constructing 3D networks.[42,43] Unfortunately, very rare candidates have been successfully developed as central cores of high-performance NFAs at present except diimide-based moieties (e.g., benzothiadiazole,[15,44] benzotriazole,[45–47] quinoxaline,[48] or phenazine[49,50] in Figure 1a). This is largely limited by the great difficulty in constructing novel heterocycles that could satisfy both specific electronic property and ease of synthesis.

For the widely used central cores of phenazine (Figure 1a), the outer electron configuration of bridging nitrogen atom (N) is 2s22p3, thereby one of the five valence electrons will remain in the p orbital perpendicular to the conjugated plane and form a featured π_6^6 system on central ring of phenazine, if the sp^2 hybridization of N atoms is adopted. Further considering the larger electronegativity (3.04) of N atom comparing to that of carbon atom (2.55), these diimide-based central cores usually exhibit the overall electron-deficient nature. In our initial concept, replacing N atom with a low valence and intrinsically strong electron-donating sulfur atom (S) may be a promising strategy to construct NIR and high-performance NFAs. Comparing to the N atom, if S atom also adopts the sp^2 hybridization

[*] Z. Xu[+], X. Cao[+], Z. Yao, W. Shi, X. Bi, Y. Li, G. Li, X. Wan, C. Li, Y. Chen
State Key Laboratory and Institute of Elemento-Organic Chemistry, The Centre of Nanoscale Science and Technology and Key Laboratory of Functional Polymer Materials, Renewable Energy Conversion and Storage Center (RECAST), College of Chemistry, Nankai University, Tianjin 300071, China
E-mail: zyao@nankai.edu.cn
yschen99@nankai.edu.cn

W. Zhao, G. Long
State Key Laboratory of Separation Membranes and Membrane Processes, School of Chemistry, Tiangong University, Tianjin 300387, China

Y. Guo
School of Materials Science and Engineering, National Institute for Advanced Materials, Renewable Energy Conversion and Storage Center (RECAST), Nankai University, Tianjin 300350, China

[+] Both authors contributed equally to this work.

Additional supporting information can be found online in the Supporting Information section

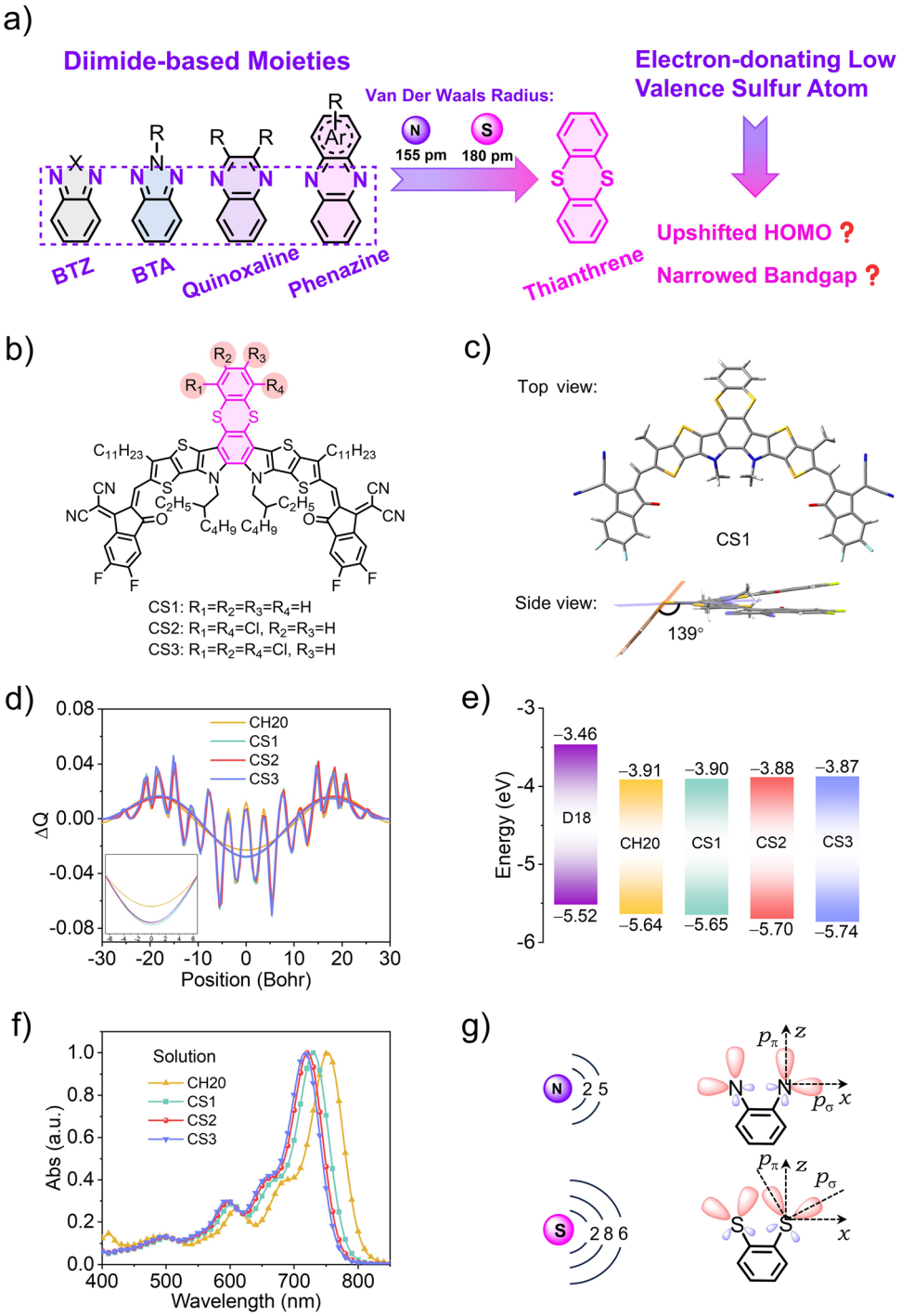

Figure 1. a) The widely reported central cores and initial concept of exploring central thianthrene. BTZ (X = S or Se): Benzothiadiazole; BTA: Benzotriazole. b) Chemical structure of CS1, CS2 and CS3. c) Theoretically simulated representative geometry of CS1. The dihedral angle of thianthrene central core was marked. d) Calculated frontier orbital charge density differences (ΔQ). e) Energy levels evaluated by cyclic voltammetry (CV). f) UV–vis spectra in solutions. g) Schematic diagram showing orientations of lone pairs on sulfur of thianthrene and nitrogen of phenazine.

that is similar to aryl dithiol, the six valence electrons of S atom would contribute to a π_6^7 conjugated system on central ring. In this way, the more electron-rich central core will upshift the highest occupied molecular orbital (HOMO) energy levels greatly and reduce the bandgaps of NFAs further,[51,52] especially when considering that S atoms possess a relatively smaller electronegativity (2.58) than N atoms. Additionally, the larger atomic radius of S (van der Waals radius: 180 pm) could theoretically increase molecular non-covalent interactions and polarizabilities that are beneficial for more compact molecular packings and efficient exciton dissociation.

Bearing these thoughts in mind, a new type of central core of thianthrene is first explored in this contribution, affording an exotic but structurally tailorable molecular platform for acceptor design. In light of the crucially important role of central halogenation in optimizing molecular packings and film morphology,[53–55] dichloro- and trichloro-substituted thianthrene were further utilized, rendering a series of NFAs, CS1, CS2, and CS3 (Figure 1b). Unexpectedly, the absorption of NFAs blue shifted significantly comparing to their diimide-based analogs, for example, CS1 versus CH20[56] (Figure S1). This phenomenon, which is completely contrary to our expectation, is mainly caused by the insufficient p–π orbital overlap of lone pair on sulfur of nonaromatic thianthrene and coterminous benzene planes. Fortunately, the desired molecular packing and fibrillary film morphology could still be achieved, especially for dichloro-substituted CS2. This finally contributed to an excellent PCE of 19.0% based on D18:CS2 blends. Our pioneer work demonstrates the enormous potential of thianthrene-based acceptors for record-breaking organic photovoltaics.

Results and Discussions

In sharp contrast to other planar central cores,[57–59] thianthrene adopts a puckered conformation with a fold angle of ~139°, unveiled by density functional theory (DFT) calculations (Figures S2 and 1c) and single crystals below. Akin to the cyclooctatetraene with 4n πe^-, thianthrene prefers a "boat" conformation[60,61] with the aim of (1) avoiding forming the unstable antiaromatic plane; the outer electron configuration of bridging S atom is $3s23p^4$, thereby two valence electrons will remain in the p orbital perpendicular to the conjugated plane and form a 4n πe^- system if the conformation is planar; (2) relieving the great ring strain; the van der Waals radius of S is 180 pm, larger than that of 155 pm for N, thereby the average C─S bond length (~1.79 Å by DFT simulation and ~1.77 Å by single crystals) in thianthrene is much larger than that of ~1.34 Å for C─N bond in phenazine. This causes a smaller C─S─C bond angle of ~100° comparing to that of ~116° for C–N–C and brings about the great ring strain (Table S1). Given the crucial role of central core in molecular packings,[62–64] the quite different packing modes from the conventional ones are expected by these NFAs owing to the puckered conformation of central core. The fluctuant ΔQ in Figure 1d is indictive of a more obvious acceptor-donor-acceptor (A-D-A) feature for CS-NFAs than CH20, which helps to facilitate charge transfer/transport while suppress charge recombination in turn.[65–67] The lowest unoccupied molecular orbitals (LUMOs) of three NFAs distribute throughout the molecular skeletons and reach the largest probability near to cyano groups while the highest occupied molecular orbitals (HOMOs) exist most on the electron-donating S, N-heteroacene with an obvious distribution on sulfur atoms of thianthrene, demonstrating the strong electron-donating feature of low valence sulfur. After central chlorination, the bandgaps increased greatly from CS1 to CS3, indicated by both DFT predication (Figure S3 and Table S2) and CV measurements (Figures 1e and S4). This results in the markedly blue-shifted absorption from CS1 to CS3, with the maximum solution/film peaks of 730/805 nm for CS1, 721/795 nm for CS2, and 717/784 nm for CS3 (Figure 1f). Note that central halogenation on NFAs could help to form a superior molecular packing network and renders the facilitated charge transfer/transport, although it usually weakens the ability of NFAs in harvesting low-energy photons.[54,68,69] However, the absorption of CS1 blue shifted significantly (22 nm in solution and 21 nm in film) comparing to its counterpart of CH20 with a phenazine central core (Figure S5 and Table S3), which is completely contrary to our initial expectation but agrees well with the DFT calculations (Figure S6). This unexpected phenomenon confuses us initially until the characteristic hybrid orbital orientation of S was unveiled. Unlike the free sulfhydryl on benzenethiol or nitrogen on phenazine that with lone pair in 3p or 2p orbitals fully overlapping with the π orbital of benzene, such a unique puckered conformation of thianthrene causes quite insufficient p–π interaction of lone pair on sulfur with coterminous benzene planes (Figure 1g),[70] which should be the root cause for this unusual absorption change above. The blue-shifted absorption of CS1 is not conducive to device performance's improvement due to the narrowed EQE response range. In addition, the differential scanning calorimetry and thermo gravimetric analysis shown in Figure S7 demonstrate the excellent thermal stability of NFAs, despite the ease of oxidation for the low valence sulfur with lone pairs.

The relatively small exciton binding energies (E_b) were roughly estimated by temperature-dependent photoluminescence (PL),[71] being 99 meV for CS1, 76 meV for CS2, and 66 meV for CS3 (Figures 2a and S8). This highlights the great effect of central halogenation on reducing E_b of NFAs,[72] and the relatively small E_bs here are conducive to efficient exciton dissociation at a low driving force. Another interesting finding is that the PL intensity of CS1 shows significant decrease compared to that of CS2 and CS3, whether in solutions or solid films (Figure S9). This conclusion was confirmed by the much larger photoluminescence quantum yields (PLQYs) for CS2 (11.8%) and CS3 (11.5%) films with respect to CS1 (0.9%) (Figures 2b and S10), additionally, the much-larger electroluminescence external quantum efficiencies of CS2 and CS3 in their neat films (Figure S11). Moreover, the PL decay curves in Figure S12 also indicate a smaller exciton lifetime of 1.19 ns for CS1 than that of 1.45 ns for CS2 and 1.42 ns for CS3. This trend is not consistent with the heavy atom effect-induced PL quenching because the halogenation occurs on outer benzene of thianthrene and the poor p–π orbital overlap between sulfur and adjacent carbon breaks the effective conjugation between outer benzene and S, N-heteroacene of NFAs. On the other hand, this may be determined by the "energy gap law"[73,74] or different excited state radiative transition probabilities.[75] It is worth noting that the undesired PL characteristic of CS1 may result in inferior exciton dissociation in resulting OSCs.[76,77]

Herein, D18 polymer[78] was selected as the donor to blend with NFAs to compose active layers of OSCs. The data of device fabrication condition screening were enumerated in Table S4–S6, with the champion J–V curves and photovoltaic

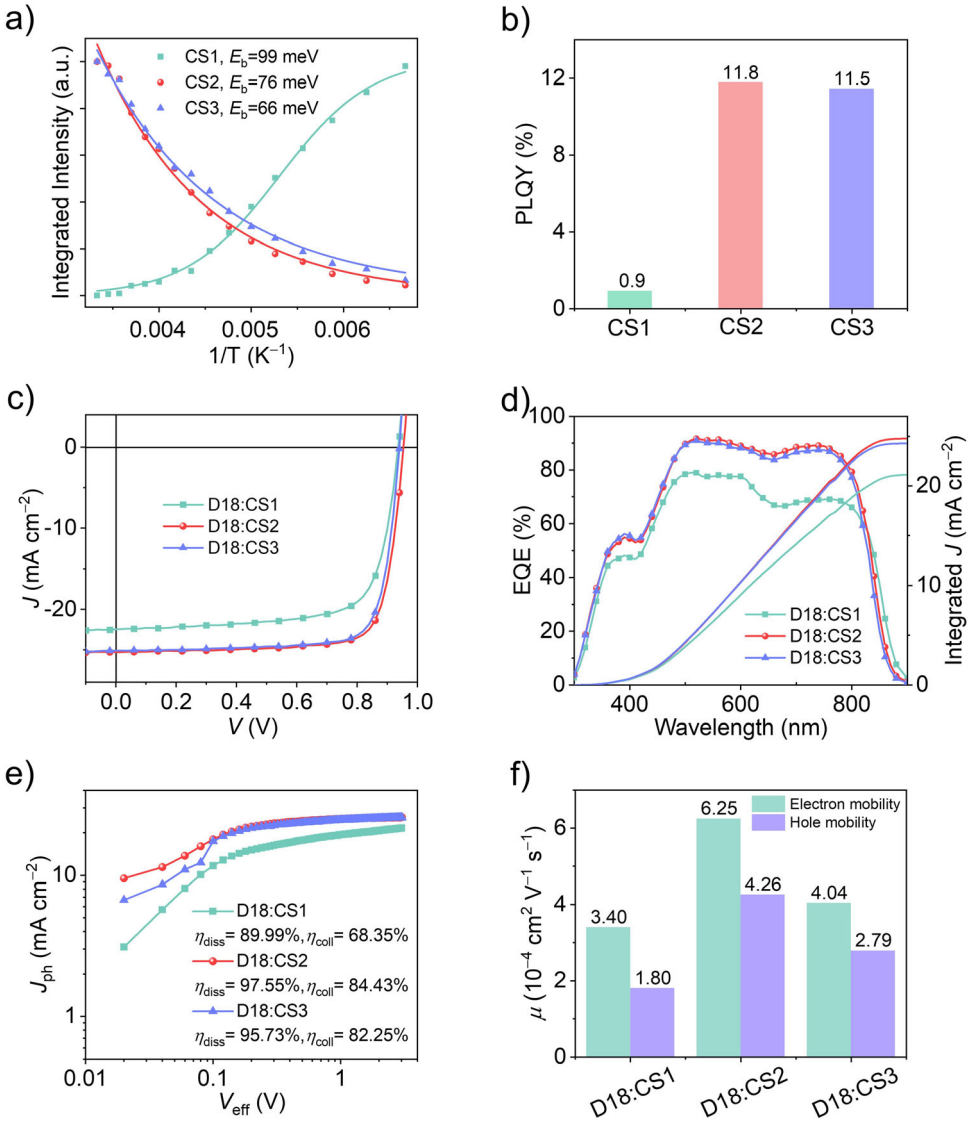

Figure 2. a) Exciton binding energies (E_b) derived from temperature-dependent PL. b) Fluorescence quantum yields (PLQYs) of NFAs in solid films. c) J–V curves. d) EQE plots. e) Saturation current density (J_{ph}) versus effective voltage (V_{eff}) curves indicating η_{diss} and η_{coll}. f) Charge mobility of blended films.

Table 1: Photovoltaic parameters for OSCs.[a)]

Active Layers	V_{OC} (V)	J_{SC} (mA cm^{-2})	Calc. J_{SC}[b)] (mA cm^{-2})	FF (%)	PCE (%)
D18:CS1	0.936 (0.938 ± 0.006)	22.47 (22.03 ± 0.26)	21.14	72.61 (69.71 ± 1.51)	15.3 (14.4 ± 0.5)
D18:CS2	0.954 (0.954 ± 0.003)	25.33 (25.13 ± 0.19)	24.78	78.63 (78.62 ± 0.38)	19.0 (18.9 ± 0.1)
D18:CS3	0.940 (0.942 ± 0.003)	25.11 (24.87 ± 0.22)	24.29	78.83 (78.68 ± 0.47)	18.6 (18.4 ± 0.1)

[a)] The best and statistical values were out/in parentheses, respectively. The statistical values were derived from 10 devices (Tables S4, S5, and S6).
[b)] Current densities afforded by EQE plots.

parameters shown in Figure 2c and Table 1, respectively. The D18:CS1-based binary OSCs afforded an outstanding open-circuit voltage (V_{OC}) of 936 mV, but unsatisfied short-circuit current density (J_{SC}) of 22.47 mA cm^{-2} and fill factor (FF) of 72.61%, thus only yielding a moderate PCE of 15.3%. After chlorination on thianthrene, a slightly enlarged V_{OC} of 954 mV, excitingly, the significantly improved J_{SC} of 25.33 mA cm^{-2} and FF of 78.63% were achieved by D18:CS2-based OSCs, affording the best PCE of 19.0%. The similar PCE enlargement could also be observed in D18:CS3-based OSCs. The J_{SC} improvement after central chlorination agrees well with the much-better external quantum efficiency (EQE) values (Figure 2d) and should mainly originate from the more efficient photodynamic processes.

Therefore, exciton dissociation (η_{diss})/charge collection (η_{coll}) efficiencies in OSCs were evaluated, being 89.99%/68.35% for CS1-, 97.55%/84.43% for CS2-, and 95.73%/82.25% for CS3-based devices (Figure 2e). Apparently, besides the inefficient charge transport in D18:CS1-based OSCs, the inferior exciton dissociation, which has been confirmed by the poorer PL quenching of D18:CS1 blends (Figure S13), should also account for the smaller J_{SC} and EQE values. This is consistent with the greatly weakened PL intensity, very low PLQY, and decreased electroluminescence EQEs of CS1 neat films as discussed above. The electron mobility (μ_e)/hole mobility (μ_h) could be determined as 3.40/1.80, 6.25/4.26, and 4.04/2.79 $\times$ 10^{-4} cm^2 V^{-1} s^{-1} for D18:CS1, D18:CS2, and D18:CS3 blends, respectively (Figures 2f and S14). The enlarged mobility along with the more balanced μ_e/μ_h ratios of CS2 and CS3 with sufficient central chlorination should account for their significantly improved FFs of OSCs. The relatively low and similar energy loss of ~0.52 eV was achieved by D18:CS1- and D18:CS2-based OSCs, which is smaller than that of ~0.55 eV for D18:CS3-based one (Table S7). The significantly downshifted HOMO energy level of CS3 guarantees the efficient exciton dissociation, however, provides excessive driving force, which causes more energy losses in turn. Therefore, for a complicated system like OSCs, it is only meaningful to reduce energy losses in the premise of efficient charge transfer/transport processes have been already achieved (see the detailed energy loss analysis in Figures S15, S16). As shown in Figure S17, all the three acceptors based OSCs possess the relatively good storage and thermal stability, despite the introduction of low-valance sulfur atoms on thianthrene.

The morphology of active layers at nanoscale largely determines the photovoltaic performance of OSCs. Therefore, we resorted to the atomic force microscopy (AFM) first to unveil the surficial morphology of D18:NFA blends (Figure S18). After central dichlorination, the more obvious fibrillary morphology was discovered in D18:CS2 blend comparing to that of D18:CS1, which is expected to facilitate the charge transport greatly in OSCs.[79,80] Thereafter, AFM coupled infrared spectroscopy (AFM-IR) was further utilized to afford a more detailed topography images that could represent donor and acceptor domains in different colors (Figure 3a). It is worth noting that D18:CS2 blend possesses a clearer fibril D/A interpenetrating morphology, comparing to that of D18:CS1 and D18:CS3. A statistical analysis revealed that D18:CS2 has the moderate and potentially suitable fibril diameter of ~14.6 nm with respect to that of ~8.5 nm for D18:CS1 and ~16.7 nm for D18:CS3 (Figures 3b and S19). This may be ascribed to the potentially effective non-covalent interactions induced by Cl···H, Cl···S, etc.,[81–83] which contributes to the weaker molecular crystallinity for CS1 but too stronger for CS3. In addition, the poorer miscibility between D18 and CS2 or CS3, which is suggested by their larger Flory–Huggins interaction parameters of χ (Figure S20 and Table S8), should also response for the enlarged fibril diameters in D18:CS2 and D18:CS3 blends.

The 2D grazing incidence wide angle X-ray scattering (GIWAXS) measurements of CS1, CS2, and CS3 neat films have disclosed the desirable face-on molecular packing orientation for three NFAs (Figure S21), moreover, revealed the stepwise increased π–π stacking distances from CS1 (3.61 Å), CS2 (3.72 Å) to CS3 (3.76 Å), which can be ascribed to the enlarged steric hindrance of central cores (Table S9). When further blending with D18 polymer, the face-on molecular packing orientation could be well maintained in three systems (Figure 3c). In contrast, D18:CS2 blend shows the smaller π–π stacking distance of 3.69 Å with respect to that of 3.76 Å for D18:CS1 and 3.74 Å for D18:CS3 (Table S10). At the same time, the molecular packing ordering in D18:CS2 blend is also improved, indicated by the slightly enlarged crystal coherence length (CCL) of 34.7 Å comparing to D18:CS1 (31.9 Å) and D18:CS3 (31.1 Å). The packing differences between neat and blended films may be caused by the more suitable miscibility between D18 and CS2, meanwhile, will benefit for the photovoltaic outcomes of resulting OSCs. The molecular crystallization dynamic was monitored by measuring in situ UV–vis absorptions. By analyzing the variation of absorption peaks, the requiring time for morphology transformation from a metastable state to a relatively stable state can be roughly delivered (Figure S22). D18:CS2 and D18:CS3 come to stable states within ~2.8 s, faster than that of D18:CS1 (~4.1 s). In short, the chloride atoms on thianthrene effectively improve the molecular crystallinity and result in the relatively larger D/A phase separation, which is beneficial for the improved FFs in D18:CS2 and D18:CS3-based OSCs.

With the aim of disclosing the effect of newly explored central thianthrene core on molecular packing, we attempted to cultivate the single crystals of NFAs (see preparing details in Supporting Information). Finally, only the single crystals of CS1 and CS2 were obtained after several trials. The single crystals have been deposited in CCDC database with a number of 2391336 for CS1 and 2391338 for CS2. Given the similar physicochemical properties and photovoltaic performances between CS2 and CS3, a firsthand comparison of CS1 and CS2 may be enough for unveiling the effects of central chlorination on thianthrene. Table S11 listed the detailed parameters for CS1 and CS2 single crystals, derived from an X-ray diffraction analysis. As shown in Figure 4a, both CS1 and CS2 have a C-shaped and helical configuration (Figure S23), more interestingly, the distinctive twist of central thianthrene with a dihedral angle of ~136°. This geometric buckling is quite different from the already reported central cores based on diimide moiety in high-performance NFAs, like Y6, CH22, AQx-2, etc.,[15,48,56,84] and may result in the unique molecular packing mode. Figure 4b exhibited the favorable 3D intermolecular packing networks for both CS1 and CS2, however, markedly distinguishing topological structure for CS2. Due to the more voids existing in crystal of CS2, a slightly decreased molecular packing coefficient of ~51.2% was estimated compared to that of ~55.3% for CS1.

As for the packing modes in crystals shown in Figure 5a,b, both CS1 and CS2 possess the typical and similar packing modes of "end-to-end" (E/E-1 and E/E-2), dual "end-to-bridge" (E/b), and "end-to-end and central-to-central" (E/E + C/C). The two types of "E/E" mode and "E/b" in CS2 show the larger average π–π stacking distances ($d_{\pi-\pi}$) comparing to that of CS1 (Table S12), agreeing with the results derived from GIWAXS measurements. Nevertheless,

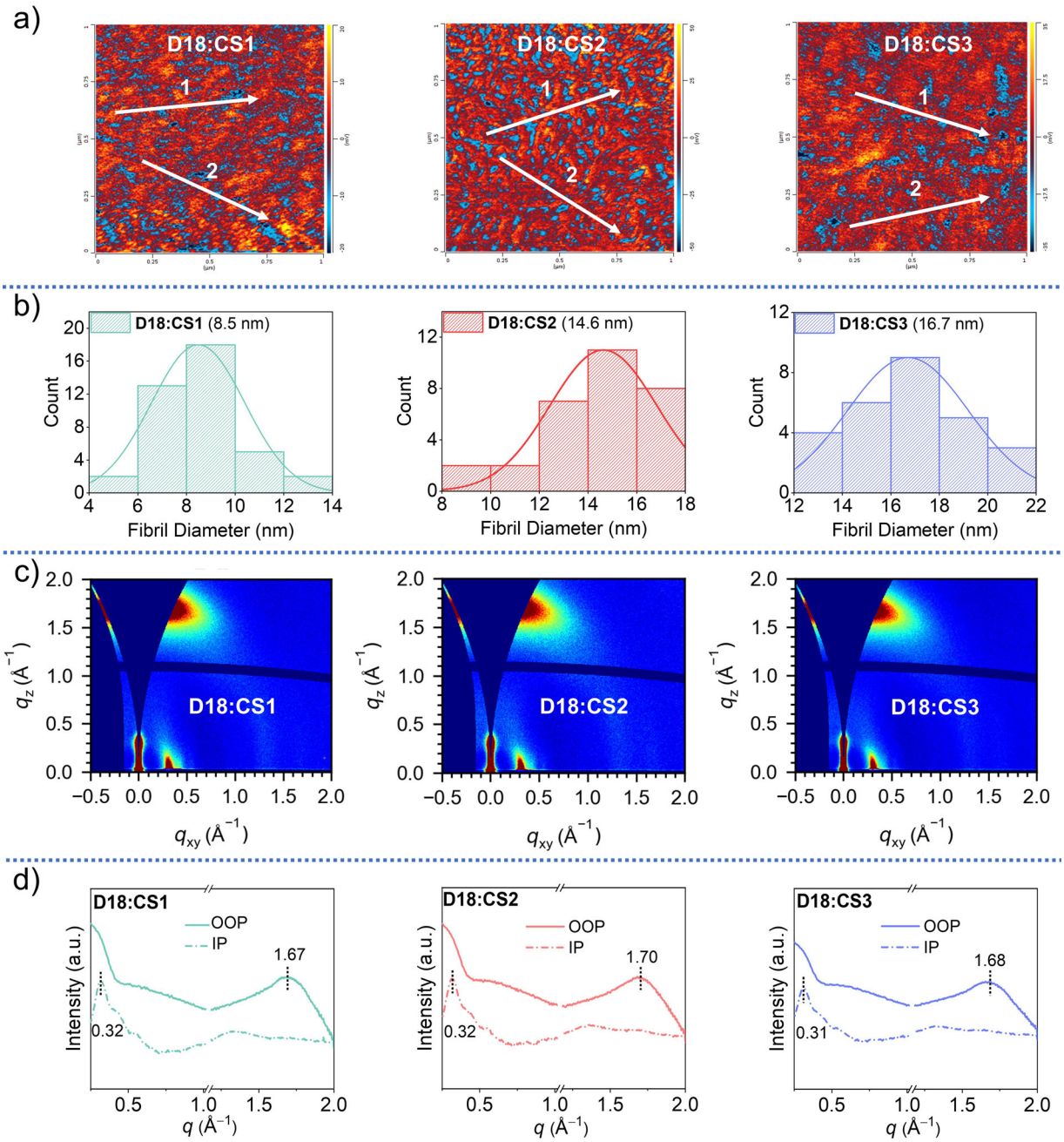

Figure 3. a) AFM-IR images of blended films. The donor and acceptor domains were marked with blue and red colors, respectively. b) Statistical phase separation sizes. c) 2D GIWAXS patterns of D18:NFA blended films. d) In-plane (IP) and out-of-plane (OOP) line-cut profiles extracted from 2D GIWAXS.

as for the "E/E + C/C" mode containing central cores, $d_{\pi\text{-}\pi}$ of CS2 (3.58 Å) becomes slightly smaller than that of CS1 (3.60 Å). In "E/E + C/C" mode, the two central units of NFAs bend in opposite directions to each other, which makes NFAs packed more tightly. At the same time, the central core that protrudes out of molecular plane also causes a large steric hindrance, spatially avoid further tight π–π stacking by a third NFA molecule. Interestingly, for the first time, a featured packing mode of "central to central" (C/C) was observed in only the CS2 crystal, with a $d_{\pi-\pi}$ of ~3.78 Å and intermolecular potential energy (E_{IP}) of 95.1 kJ mol^{-1}. This "C/C" mode was achieved by stacking the outer benzene rings of folded thianthrene together. Due to the almost no orbital overlap between the outer benzene and main conjugated S, N-heteroacene, the electron transfer integral of "C/C" mode is near to zero, which suggests that the outer benzene of thianthrene has limited effects on charge transport of NFAs but may still play an important role in constructing the unique 3D molecular packing network of CS2 (just like working as another end unit with the nonaromatic feature). The intermolecular potential energies (E_{IP}) of "E/b + E/C" mode in CS1 and CS2 are ~91.9 and ~91.2 kJ mol^{-1}, but the

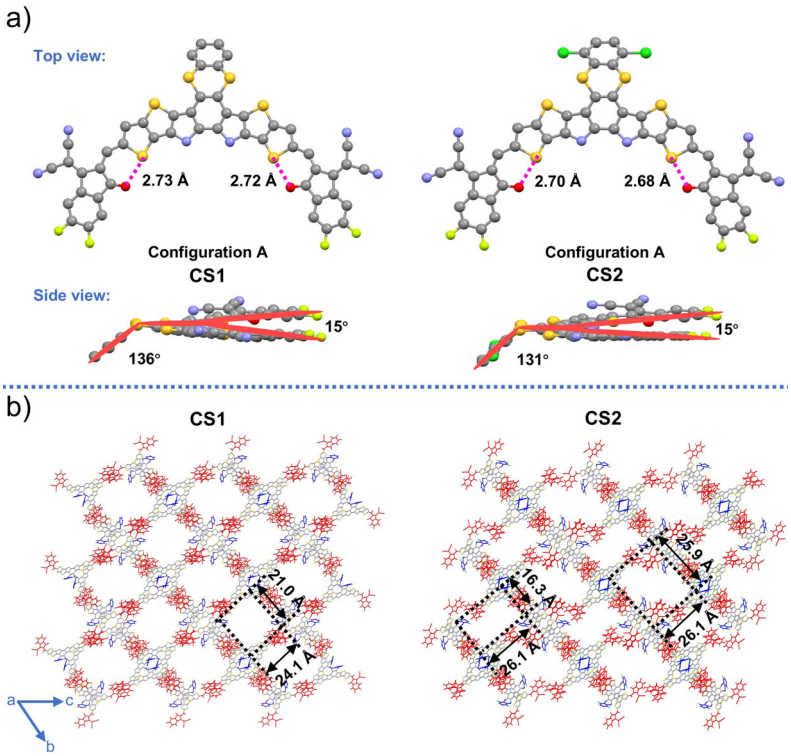

Figure 4. a) Single crystal geometries of CS1 and CS2 from both top and side view. The twisted angles of central thianthrene core were also marked. b) Molecular packing topological structures in CS1 and CS2 crystals from the top view.

$d_{\pi-\pi}$ are as large as 7.91 and 6.66 Å, respectively. Such a $d_{\pi-\pi}$ is greatly larger than the typical $d_{\pi-\pi}$ of 3.3–3.8 Å, suggesting the strong entanglement of alkyl chains rather than π–π stacking interactions. The effect of chain entanglement on molecular stacking pattern proves that the carefully regulating side chains will certainly optimize molecular stacking behavior and boost photovoltaic performance better for thianthrene-based NFAs, just as the great success in side chain engineering of Y6.[85–87] It is also worth noting that although CS1 possesses a puckered central core of thianthrene, its average $d_{\pi-\pi}$ (with π–π stacking interaction) of ~3.41 Å is comparable to that of ~3.42 Å for CH20 with a planar phenazine central core (Figure S24). Moreover, the excellent charge transfer could still be achieved by CS1 comparing to CH20, which could be confirmed by their comparable electronic transfer integrals for packing modes with the maximum intermolecular potentials and experimentally measured electron mobility (Table S13). This should be one of the reasons that nonplanar backbone of thianthrene-based NFAs can also achieve a high-performance OSC. In order to better compare with classical acceptors in the field, we have compared CS2 with Y6 and CH23 comprehensively (Figure S25) and built a detailed Table S14 to afford a clear landscape of their physicochemical properties at both central units and acceptors levels. It is worth noting that the physicochemical properties of CS2 with the thianthrene central unit exhibit significant differences from Y6 and CH23 with benzothiadiazole and phenazine, respectively, which further highlights the innovativeness of thianthrene based molecular platform developed here.

Conclusion

A new concept central core of nonaromatic thianthrene is explored for the first time, affording an exotic but structurally tailorable molecular platform for NFAs design. After further central chlorination, three novel NFAs of CS1, CS2, and CS3 were afforded with suitable energy levels and absorptions, relatively small E_b and good material thermal stability, etc. Note that the thianthrene central core prefers a unique puckered or "boat" conformation with the aim of avoiding forming the unstable antiaromatic plane with 4n πe^- and relieving the great ring strain, thus resulting in the quite insufficient p–π orbital overlap between lone pair on sulfur of thianthrene and the coterminous benzene planes. This is in sharp contrast to the nitrogen atoms on benzothiadiazole, quinoxaline, phenazine, etc. that with lone pair in 2p orbital fully overlapping with the π orbital of benzene. Therefore, regardless of the highly strong electron-donating characteristic of low valence sulfur, the absorption of CS-NFAs shows the unexpected but obvious blue-shifting compared to the counterpart of CH20 with phenazine central core. A detailed single crystal analysis revealed (1) the bent geometry of central core does not damage the desired 3D intermolecular packing networks, which may be contrary to the popular belief; (2) after central chlorination, a rarely observed "C/C" mode was achieved in CS2 by stacking the outer benzene of thianthrene together. Note that the outer benzene of thianthrene has limited effects on charge transport of NFAs but may work as another nonaromatic

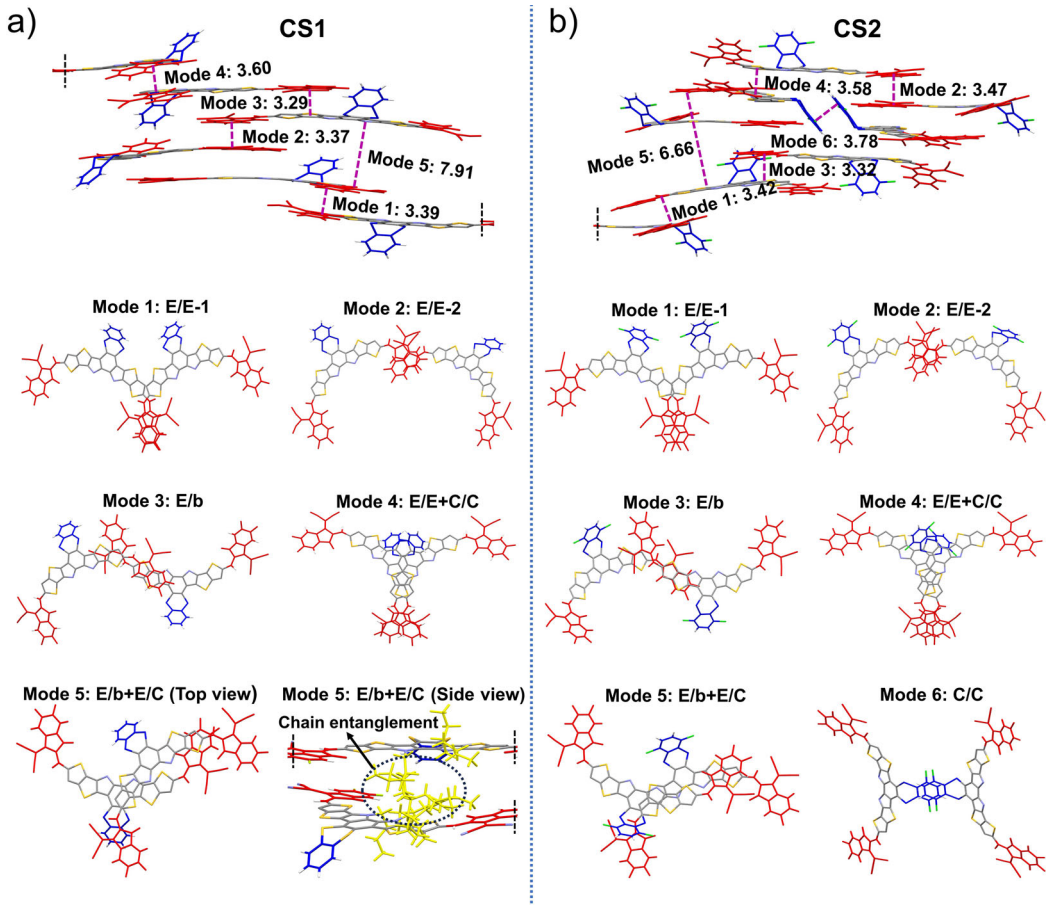

Figure 5. The main intermolecular packing modes in CS1 and CS2 crystals with intermolecular potential energies over 70 kJ mol^{-1}. Note that the puckered conformation results in over twenty molecular packing modes with only subtle differences. Herein, only the modes, which directly dominate the formation of 3D packing networks, were presented. a) Packing modes in CS1. b) Packing modes in CS2.

end unit and play an important role in constructing the unique 3D molecular packing network of CS2; (3) the widely existed chain entanglement in both CS1 and CS2 crystals suggests the great potential of CS-NFAs for achieving better photovoltaic performance by means of further side chain engineering, just like the classic Y6. Moreover, benefitting from the proper central chlorination, the desired fibrillary morphology of blended films with suitable D/A phase separation was achieved, especially for D18:CS2 blends. As a result, binary OSCs based on D18:CS2 rendered the best device efficiency of 19.0%, which ranks among the first-class binary organic photovoltaic devices. Our works will undoubtedly stimulate more structural optimization on such an innovative molecular platform with a thianthrene central core, for example, potentially developing radical cations of thianthrene due to its easy and reversible oxidation, but relatively stable features; or utilizing the poor p–π orbital overlap to explore NFAs with thermal active delay fluorescent features, by introducing super electron-donating groups on outer benzene of central thianthrene, etc. At the same time, our successful trials on thianthrene core will also boost extensive investigations on other promising central structures.

Supporting Information

The Supporting Information is available free of charge, including materials synthesis (Scheme S1–S5), device characterization and stability measurements, charge mobility, CV, UV-vis spectra, NMR and HR-MS spectra (Figure S1–S49), additional tables, *etc*.

Acknowledgements

The authors gratefully acknowledge the financial support from Ministry of Science and Technology of the People's Republic of China (National Key R&D Program of China, 2023YFE0210400), National Natural Science Foundation of China (22309090, 22479081, 21935007, 52025033, 51873089, 22204119, 22361132530, 52373189), and Natural Science Foundation of Tianjin (23JCZDJC01160).

Conflict of Interests

The authors declare no conflict of interest.

Data Availability Statement

The data that support the findings of this study are available from the corresponding author upon reasonable request.

Keywords: Non-fullerene acceptors · Organic photovoltaic · Puckered central core · P–π conjugation · Thianthrene

[1] C. Chen, L. Wang, W. Xia, K. Qiu, C. Guo, Z. Gan, J. Zhou, Y. Sun, D. Liu, W. Li, T. Wang, *Nat. Commun.* **2024**, *15*, 6865.

[2] Z. Chen, J. Ge, W. Song, X. Tong, H. Liu, X. Yu, J. Li, J. Shi, L. Xie, C. Han, Q. Liu, Z. Ge, *Adv. Mater.* **2024**, *36*, 2406690.

[3] Z. Ge, J. Qiao, Y. Li, J. Song, X. Duan, Z. Fu, H. Hu, R. Yang, H. Yin, X. Hao, Y. Sun, *Angew. Chem. Int. Ed.* **2024**, e202413309.

[4] S. Guan, Y. Li, C. Xu, N. Yin, C. Xu, C. Wang, M. Wang, Y. Xu, Q. Chen, D. Wang, L. Zuo, H. Chen, *Adv. Mater.* **2024**, *36*, 2400342.

[5] Y. Jiang, S. Sun, R. Xu, F. Liu, X. Miao, G. Ran, K. Liu, Y. Yi, W. Zhang, X. Zhu, *Nat. Energy* **2024**, *9*, 975–986.

[6] C. Li, G. Yao, X. Gu, J. Lv, Y. Hou, Q. Lin, N. Yu, M. S. Abbasi, X. Zhang, J. Zhang, Z. Tang, Q. Peng, C. Zhang, Y. Cai, H. Huang, *Nat. Commun.* **2024**, *15*, 8872.

[7] H. Lu, D. Li, W. Liu, G. Ran, H. Wu, N. Wei, Z. Tang, Y. Liu, W. Zhang, Z. Bo, *Angew. Chem. Int. Ed.* **2024**, *63*, e202407007.

[8] Y. Sun, L. Wang, C. Guo, J. Xiao, C. Liu, C. Chen, W. Xia, Z. Gan, J. Cheng, J. Zhou, Z. Chen, J. Zhou, D. Liu, T. Wang, W. Li, *J. Am. Chem. Soc.* **2024**, *146*, 12011–12019.

[9] N. Wei, J. Chen, Y. Cheng, Z. Bian, W. Liu, H. Song, Y. Guo, W. Zhang, Y. Liu, H. Lu, J. Zhou, Z. Bo, *Adv. Mater.* **2024**, *36*, 2408934.

[10] Y. Yu, J. Wang, Z. Chen, Y. Xiao, Z. Fu, T. Zhang, H. Yuan, X.-T. Hao, L. Ye, Y. Cui, J. Hou, *Sci. China Chem.* **2024**, *67*, 4194–4201.

[11] L. Zhu, M. Zhang, G. Zhou, Z. Wang, W. Zhong, J. Zhuang, Z. Zhou, X. Gao, L. Kan, B. Hao, F. Han, R. Zeng, X. Xue, S. Xu, H. Jing, B. Xiao, H. Zhu, Y. Zhang, F. Liu, *Joule* **2024**, *8*, 3153–3168.

[12] Y.-J. Xue, Z.-Y. Lai, H.-C. Lu, J.-C. Hong, C.-L. Tsai, C.-L. Huang, K.-H. Huang, C.-F. Lu, Y.-Y. Lai, C.-S. Hsu, J.-M. Lin, J.-W. Chang, S.-Y. Chien, G.-H. Lee, U. S. Jeng, Y.-J. Cheng, *J. Am. Chem. Soc.* **2024**, *146*, 833–848.

[13] H. W. Kroto, J. R. Heath, S. C. O'Brien, R. F. Curl, R. E. Smalley, *Nature* **1985**, *318*, 162–163.

[14] Y. Lin, J. Wang, Z.-G. Zhang, H. Bai, Y. Li, D. Zhu, X. Zhan, *Adv. Mater.* **2015**, *27*, 1170–1174.

[15] J. Yuan, Y. Zhang, L. Zhou, G. Zhang, H.-L. Yip, T.-K. Lau, X. Lu, C. Zhu, H. Peng, P. A. Johnson, M. Leclerc, Y. Cao, J. Ulanski, Y. Li, Y. Zou, *Joule* **2019**, *3*, 1140–1151.

[16] J. Benduhn, K. Tvingstedt, F. Piersimoni, S. Ullbrich, Y. Fan, M. Tropiano, K. A. McGarry, O. Zeika, M. K. Riede, C. J. Douglas, S. Barlow, S. R. Marder, D. Neher, D. Spoltore, K. Vandewal, *Nat. Energy* **2017**, *2*, 17053.

[17] G. Yu, J. Gao, J. C. Hummelen, F. Wudl, A. J. Heeger, *Science* **1995**, *270*, 1789–1791.

[18] C. Duan, L. Ding, *Sci. Bull.* **2020**, *65*, 1231–1233.

[19] J. Cao, L. Yi, L. Ding, *J. Semicond.* **2022**, *43*, 030202.

[20] R. Zeng, M. Zhang, X. Wang, L. Zhu, B. Hao, W. Zhong, G. Zhou, J. Deng, S. Tan, J. Zhuang, F. Han, A. Zhang, Z. Zhou, X. Xue, S. Xu, J. Xu, Y. Liu, H. Lu, X. Wu, C. Wang, Z. Fink, T. P. Russell, H. Jing, Y. Zhang, Z. Bo, F. Liu, *Nat. Energy* **2024**, *9*, 1117–1128.

[21] R. Xu, Y. Jiang, F. Liu, G. Ran, K. Liu, W. Zhang, X. Zhu, *Adv. Mater.* **2024**, *36*, 2312101.

[22] Y. Ma, D. Cai, S. Wan, P. Wang, J. Wang, Q. Zheng, *Angew. Chem. Int. Ed.* **2020**, *59*, 21627–21633.

[23] M. Zhang, L. Zhu, G. Zhou, T. Hao, C. Qiu, Z. Zhao, Q. Hu, B. W. Larson, H. Zhu, Z. Ma, Z. Tang, W. Feng, Y. Zhang, T. P. Russell, F. Liu, *Nat. Commun.* **2021**, *12*, 309.

[24] D. Beljonne, G. Pourtois, C. Silva, E. Hennebicq, L. M. Herz, R. H. Friend, G. D. Scholes, S. Setayesh, K. Müllen, J. L. Brédas, *Proc. Natl. Acad. Sci. USA* **2002**, *99*, 10982–10987.

[25] W. Zhu, A. P. Spencer, S. Mukherjee, J. M. Alzola, V. K. Sangwan, S. H. Amsterdam, S. M. Swick, L. O. Jones, M. C. Heiber, A. A. Herzing, G. Li, C. L. Stern, D. M. DeLongchamp, K. L. Kohlstedt, M. C. Hersam, G. C. Schatz, M. R. Wasielewski, L. X. Chen, A. Facchetti, T. J. Marks, *J. Am. Chem. Soc.* **2020**, *142*, 14532–14547.

[26] Z. Jia, S. Qin, L. Meng, Q. Ma, I. Angunawela, J. Zhang, X. Li, Y. He, W. Lai, N. Li, H. Ade, C. J. Brabec, Y. Li, *Nat. Commun.* **2021**, *12*, 178.

[27] L. Meng, Y. Zhang, X. Wan, C. Li, X. Zhang, Y. Wang, X. Ke, Z. Xiao, L. Ding, R. Xia, H.-L. Yip, Y. Cao, Y. Chen, *Science* **2018**, *361*, 1094–1098.

[28] Z. Zheng, J. Wang, P. Bi, J. Ren, Y. Wang, Y. Yang, X. Liu, S. Zhang, J. Hou, *Joule* **2022**, *6*, 171–184.

[29] J. Wang, Z. Zheng, P. Bi, Z. Chen, Y. Wang, X. Liu, S. Zhang, X. Hao, M. Zhang, Y. Li, J. Hou, *Natl. Sci. Rev.* **2023**, *10*, nwad085.

[30] Y.-C. Wei, S. F. Wang, Y. Hu, L.-S. Liao, D.-G. Chen, K.-H. Chang, C.-W. Wang, S.-H. Liu, W.-H. Chan, J.-L. Liao, W.-Y. Hung, T.-H. Wang, P.-T. Chen, H.-F. Hsu, Y. Chi, P.-T. Chou, *Nat. Commun.* **2020**, *14*, 570–577.

[31] C. Erker, T. Basché, *J. Am. Chem. Soc.* **2022**, *144*, 14053–14056.

[32] T. Duan, W. Feng, Y. Li, Z. Li, Z. Zhang, H. Liang, H. Chen, C. Zhong, S. Jeong, C. Yang, S. Chen, S. Lu, O. A. Rakitin, C. Li, X. Wan, B. Kan, Y. Chen, *Angew. Chem. Int. Ed.* **2023**, *62*, e202308832.

[33] J. Fu, Q. Yang, P. Huang, S. Chung, K. Cho, Z. Kan, H. Liu, X. Lu, Y. Lang, H. Lai, F. He, P. W. K. Fong, S. Lu, Y. Yang, Z. Xiao, G. Li, *Nat. Commun.* **2024**, *15*, 1830.

[34] X. Meng, M. Li, K. Jin, L. Zhang, J. Sun, W. Zhang, C. Yi, J. Yang, F. Hao, G.-W. Wang, Z. Xiao, L. Ding, *Angew. Chem. Int. Ed.* **2022**, *61*, e202207762.

[35] S.-F. Wang, B.-K. Su, X.-Q. Wang, Y.-C. Wei, K.-H. Kuo, C.-H. Wang, S.-H. Liu, L.-S. Liao, W.-Y. Hung, L.-W. Fu, W.-T. Chuang, M. Qin, X. Lu, C. You, Y. Chi, P.-T. Chou, *Nat. Photonics* **2022**, *16*, 843–850.

[36] Y.-C. Wei, K.-H. Kuo, Y. Chi, P.-T. Chou, *Acc. Chem. Res.* **2023**, *56*, 689–699.

[37] S.-F. Wang, D.-Y. Zhou, K.-H. Kuo, C.-H. Wang, C.-M. Hung, J. Yan, L.-S. Liao, W.-Y. Hung, Y. Chi, P.-T. Chou, *Angew. Chem. Int. Ed.* **2024**, *63*, e202317571.

[38] C. Tang, X. Ma, J.-Y. Wang, X. Zhang, R. Liao, Y. Ma, P. Wang, P. Wang, T. Wang, F. Zhang, Q. Zheng, *Angew. Chem. Int. Ed.* **2021**, *60*, 19314–19323.

[39] T. Chen, S. Li, Y. Li, Z. Chen, H. Wu, Y. Lin, Y. Gao, M. Wang, G. Ding, J. Min, Z. Ma, H. Zhu, L. Zuo, H. Chen, *Adv. Mater.* **2023**, *35*, 2300400.

[40] L. Chen, C. Zhao, H. Yu, A. Sergeev, L. Zhu, K. Ding, Y. Fu, H. M. Ng, C. H. Kwok, X. Zou, J. Yi, X. Lu, K. S. Wong, H. Ade, G. Zhang, H. Yan, *Adv. Energy Mater.* **2024**, *14*, 2400285.

[41] Y. Zou, H. Chen, X. Bi, X. Xu, H. Wang, M. Lin, Z. Ma, M. Zhang, C. Li, X. Wan, G. Long, Y. Zhaoyang, Y. Chen, *Energy Environ. Sci.* **2022**, *15*, 3519–3533.

[42] X. Li, R. Peng, Y. Qiu, Y. Zhang, J. Shi, S. Gao, H. Liu, F. Jin, Z. Ge, *Adv. Funct. Mater.* **2024**, *35* 2413259.

[43] D. Qiu, H. Zhang, C. Tian, J. Zhang, L. Zhu, Z. Wei, K. Lu, *Adv. Mater.* **2023**, *35*, 2307398.

[44] Z. Zhang, Y. Li, G. Cai, Y. Zhang, X. Lu, Y. Lin, *J. Am. Chem. Soc.* **2020**, *142*, 18741–18745.

[45] C. Zhu, J. Yuan, F. Cai, L. Meng, H. Zhang, H. Chen, J. Li, B. Qiu, H. Peng, S. Chen, Y. Hu, C. Yang, F. Gao, Y. Zou, Y. Li, *Energy Environ. Sci.* **2020**, *13*, 2459–2466.

[46] L. Zhou, H. Yu, J. Zhang, D. Qiu, Y. Fu, J. Yi, L. Xie, X. Li, L. Meng, J. Zhang, X. Lu, Z. Wei, Y. Li, H. Yan, *Angew. Chem. Int. Ed.* **2024**, *63*, e202319635.
[47] H. He, X. Li, J. Zhang, Z. Chen, Y. Gong, H. Zhuo, X. Wu, Y. Li, S. Wang, Z. Bi, B. Song, K. Zhou, T. Liang, W. Ma, G. Lu, L. Ye, L. Meng, B. Zhang, Y. Li, Y. Li, *Nat. Commun.* **2025**, *16*, 787.
[48] Z. Zhou, W. Liu, G. Zhou, M. Zhang, D. Qian, J. Zhang, S. Chen, S. Xu, C. Yang, F. Gao, H. Zhu, F. Liu, X. Zhu, *Adv. Mater.* **2020**, *32*, 1906324.
[49] Y. Shi, Y. Chang, K. Lu, Z. Chen, J. Zhang, Y. Yan, D. Qiu, Y. Liu, M. A. Adil, W. Ma, X. Hao, L. Zhu, Z. Wei, *Nat. Commun.* **2022**, *13*, 3256.
[50] H. Chen, H. Liang, Z. Guo, Y. Zhu, Z. Zhang, Z. Li, X. Cao, H. Wang, W. Feng, Y. Zou, L. Meng, X. Xu, B. Kan, C. Li, Z. Yao, X. Wan, Z. Ma, Y. Chen, *Angew. Chem. Int. Ed.* **2022**, *61*, e202209580.
[51] P. Li, X. Meng, K. Jin, Z. Xu, J. Zhang, L. Zhang, C. Niu, F. Tan, C. Yi, Z. Xiao, Y. Feng, G.-W. Wang, L. Ding, *Carbon Energy* **2023**, *5*, e250.
[52] W. Wei, X. Yuan, J. Zhong, Z. Wang, X. Zhou, F. Zhao, D. Feng, Y. Zhang, W. Chen, M. Yang, W. Zhang, Z. Ma, Z. Tang, X. Lu, F. Huang, Y. Cao, C. Duan, *Energy Environ. Sci.* **2024**, *17*, 6627–6639.
[53] Z. Yao, X. Cao, X. Bi, T. He, Y. Li, X. Jia, H. Liang, Y. Guo, G. Long, B. Kan, C. Li, X. Wan, Y. Chen, *Angew. Chem. Int. Ed.* **2023**, *62*, e202312630.
[54] T. Xu, Z. Luo, R. Ma, Z. Chen, T. A. Dela Peña, H. Liu, Q. Wei, M. Li, C. e. Zhang, J. Wu, X. Lu, G. Li, C. Yang, *Angew. Chem. Int. Ed.* **2023**, *62*, e202304127.
[55] K. Liu, Y. Jiang, G. Ran, F. Liu, W. Zhang, X. Zhu, *Joule* **2024**, *8*, 835–851.
[56] H. Liang, X. Bi, H. Chen, T. He, Y. Lin, Y. Zhang, K. Ma, W. Feng, Z. Ma, G. Long, C. Li, B. Kan, H. Zhang, O. A. Rakitin, X. Wan, Z. Yao, Y. Chen, *Nat. Commun.* **2023**, *14*, 4707.
[57] X. Li, S. Luo, H. Sun, H. H.-Y. Sung, H. Yu, T. Liu, Y. Xiao, F. Bai, M. Pan, X. Lu, I. D. Williams, X. Guo, Y. Li, H. Yan, *Energy Environ. Sci.* **2021**, *14*, 4555–4563.
[58] M. Deng, X. Xu, Y. Duan, W. Qiu, L. Yu, R. Li, Q. Peng, *Adv. Mater.* **2024**, *36*, 2308216.
[59] C. He, Y. Pan, Y. Ouyang, Q. Shen, Y. Gao, K. Yan, J. Fang, Y. Chen, C.-Q. Ma, J. Min, C. Zhang, L. Zuo, H. Chen, *Energy Environ. Sci.* **2022**, *15*, 2537–2544.
[60] S. I. Etkind, T. M. Swager, *Synthesis* **2022**, *54*, 4843–4863.
[61] O. Y. Borbulevych, O. V. Shishkin, *J. Mol. Struct.* **1998**, *446*, 11–14.
[62] H. Liu, Y. Geng, Z. Xiao, L. Ding, J. Du, A. Tang, E. Zhou, *Adv. Mater.* **2024**, *36*, 2404660.
[63] Z. Yao, X. Wan, C. Li, Y. Chen, *Acc. Mater.* **2023**, *4*, 772–785.
[64] M. Li, W. A. Memon, S. Xiong, Y. Ding, Y. Wang, H. Li, J. Si, L. Tian, F. He, *Energy Environ. Sci.* **2024**, *17*, 7895–7907.
[65] L. Wang, Q. An, L. Yan, H.-R. Bai, M. Jiang, A. Mahmood, C. Yang, H. Zhi, J.-L. Wang, *Energy Environ. Sci.* **2022**, *15*, 320–333.
[66] H. Yu, Y. Wang, X. Zou, H. Han, H. K. Kim, Z. Yao, Z. Wang, Y. Li, H. M. Ng, W. Zhou, J. Zhang, S. Chen, X. Lu, K. S. Wong, Z. Zhu, H. Yan, H. Hu, *Adv. Funct. Mater.* **2023**, *33*, 2300712.
[67] X. Zhang, G. Li, S. Mukherjee, W. Huang, D. Zheng, L.-W. Feng, Y. Chen, J. Wu, V. K. Sangwan, M. C. Hersam, D. M. DeLongchamp, J. Yu, A. Facchetti, T. J. Marks, *Adv. Energy Mater.* **2022**, *12*, 2102172.
[68] Z. Luo, W. Wei, R. Ma, G. Ran, M. H. Jee, Z. Chen, Y. Li, W. Zhang, H. Y. Woo, C. Yang, *Adv. Mater.* **2024**, *36*, 2407517.
[69] Y. Gong, T. Zou, X. Li, S. Qin, G. Sun, T. Liang, R. Zhou, J. Zhang, J. Zhang, L. Meng, Z. Wei, Y. Li, *Energy Environ. Sci.* **2024**, *17*, 6844–6855.
[70] S. Kim, Y. Kwon, J.-P. Lee, S.-Y. Choi, J. Choo, *J. Mol. Struct.* **2003**, *655*, 451–458.
[71] L. Zhu, J. Zhang, Y. Guo, C. Yang, Y. Yi, Z. Wei, *Angew. Chem. Int. Ed.* **2021**, *60*, 15348–15353.
[72] A. Ashokan, T. Wang, M. K. Ravva, J.-L. Brédas, *J. Mater. Chem. C* **2018**, *6*, 13162–13170.
[73] J. S. Wilson, N. Chawdhury, M. R. A. Al-Mandhary, M. Younus, M. S. Khan, P. R. Raithby, A. Köhler, R. H. Friend, *J. Am. Chem. Soc.* **2001**, *123*, 9412–9417.
[74] D. Yang, J. Huang, X. Hu, H. Guo, D. Xie, *Nat. Commun.* **2019**, *10*, 4658.
[75] M. Zhang, Z. Yao, C. Yan, Y. Cai, Y. Ren, J. Zhang, P. Wang, *ACS Photonics* **2014**, *1*, 710–717.
[76] W. Wang, J. Wang, Y. Cui, Z. Li, J. Wang, C. Wang, Z. Chen, J. Qiao, X. Hao, J. Hou, *Adv. Energy Mater.* **2024**, *14*, 2303605.
[77] D. Qian, Z. Zheng, H. Yao, W. Tress, T. R. Hopper, S. Chen, S. Li, J. Liu, S. Chen, J. Zhang, X.-K. Liu, B. Gao, L. Ouyang, Y. Jin, G. Pozina, I. A. Buyanova, W. M. Chen, O. Inganäs, V. Coropceanu, J.-L. Bredas, H. Yan, J. Hou, F. Zhang, A. A. Bakulin, F. Gao, *Nat. Mater.* **2018**, *17*, 703–709.
[78] Q. Liu, Y. Jiang, K. Jin, J. Qin, J. Xu, W. Li, J. Xiong, J. Liu, Z. Xiao, K. Sun, S. Yang, X. Zhang, L. Ding, *Sci. Bull.* **2020**, *65*, 272–275.
[79] X. Song, L. Mei, X. Zhou, H. Li, H. Xu, X. Liu, S. Gao, S. Xu, Y. Yang, W. Zhu, J. Wang, X.-H. Zhang, X.-K. Chen, *Angew. Chem. Int. Ed.* **2024**, *63* e202411512.
[80] L. Zhu, M. Zhang, J. Xu, C. Li, J. Yan, G. Zhou, W. Zhong, T. Hao, J. Song, X. Xue, Z. Zhou, R. Zeng, H. Zhu, C.-C. Chen, R. C. I. MacKenzie, Y. Zou, J. Nelson, Y. Zhang, Y. Sun, F. Liu, *Nat. Mater.* **2022**, *21*, 656–663.
[81] C. Guan, C. Xiao, X. Liu, Z. Hu, R. Wang, C. Wang, C. Xie, Z. Cai, W. Li, *Angew. Chem. Int. Ed.* **2023**, *62*, e202312357.
[82] W. Gao, R. Ma, T. A. Dela Peña, C. Yan, H. Li, M. Li, J. Wu, P. Cheng, C. Zhong, Z. Wei, A. K. Y. Jen, G. Li, *Nat. Commun.* **2024**, *15*, 1946.
[83] F. Cheng, Y. Cui, F. Ding, Z. Chen, Q. Xie, X. Xia, P. Zhu, X. Lu, H. Zhu, X. Liao, Y. Chen, *Adv. Mater.* **2023**, *35*, 2300820.
[84] J. Yuan, T. Huang, P. Cheng, Y. Zou, H. Zhang, J. L. Yang, S.-Y. Chang, Z. Zhang, W. Huang, R. Wang, D. Meng, F. Gao, Y. Yang, *Nat. Commun.* **2019**, *10*, 570.
[85] Y. Cui, H. Yao, J. Zhang, K. Xian, T. Zhang, L. Hong, Y. Wang, Y. Xu, K. Ma, C. An, C. He, Z. Wei, F. Gao, J. Hou, *Adv. Mater.* **2020**, *32*, 1908205.
[86] C. Li, J. Zhou, J. Song, J. Xu, H. Zhang, X. Zhang, J. Guo, L. Zhu, D. Wei, G. Han, J. Min, Y. Zhang, Z. Xie, Y. Yi, H. Yan, F. Gao, F. Liu, Y. Sun, *Nat. Energy* **2021**, *6*, 605–613.
[87] B. Fan, W. Gao, R. Zhang, W. Kaminsky, F. R. Lin, X. Xia, Q. Fan, Y. Li, Y. An, Y. Wu, M. Liu, X. Lu, W. J. Li, H.-L. Yip, F. Gao, A. K. Y. Jen, *J. Am. Chem. Soc.* **2023**, *145*, 5909–5919.

Manuscript received: November 02, 2024
Revised manuscript received: March 11, 2025
Accepted manuscript online: March 24, 2025
Version of record online: ■■, ■■

Research Article

Organic Photovoltaics

Z. Xu, X. Cao, Z. Yao*, W. Zhao, W. Shi, X. Bi, Y. Li, Y. Guo, G. Li, G. Long, X. Wan, C. Li, Y. Chen* — **e202421289**

Highly Efficient Acceptors with a Nonaromatic Thianthrene Central Core for Organic Photovoltaics

A new concept central core of nonaromatic thianthrene is explored for the first time, affording an exotic but structurally tailorable molecular platform for NFAs design.